

1 **Combined influence of maximum accumulation and melt rates on the 2 duration of the seasonal snowpack over temperate mountains**

3 Esteban Alonso-González¹, Jesús Revuelto¹ Steven R. Fassnacht^{2,3,4}, Juan Ignacio López-Moreno¹

4
5 1- Instituto Pirenaico de Ecología, Spanish Research Council (IPE-CSIC), Zaragoza, Spain.

6 2- ESS-Watershed Science, Colorado State University, Fort Collins, CO 80523, USA.

7 3- Natural Resources Ecology Laboratory, Fort Collins, CO 80523, USA.

8 4- Cooperative Institute for Research in the Atmosphere, Fort Collins, CO 80523, USA.

9 **Abstract**

10 The duration of the seasonal snowpack determines numerous aspects of the water cycle, ecology
11 and the economy in cold and mountainous regions, and is a balance between the magnitude of
12 accumulated snow and the rate of melt. The contribution of each component has not been well
13 quantified under contrasting topography and climatological conditions although this may provide
14 useful insights into how snow cover duration could respond to climate change. Here, we examined
15 the contribution of the annual peak snow water equivalent (SWE) and the seasonal melt rate to
16 define the duration of the snowpack over temperate mountains, using snow data for mountain areas
17 with different climatological characteristics across the Iberian Peninsula. We used a daily snowpack
18 database for the period 1980–2014 over Iberia to derive the seasonal peak SWE, melt rate and
19 season snow cover duration. The influence of peak SWE and melt rates on seasonal snow cover
20 duration was estimated using a stepwise linear model approach.

21 The stepwise linear models showed high R-adjusted values (average R-adjusted = 0.7), without any
22 clear dependence on the elevation or geographical location. In general, the peak SWE influenced
23 the snow cover duration over all of the mountain areas analysed to a greater extent than the melt
24 rates (89.1%, 89.2%, 81.6% 93.2% and 95.5% in the areas for the Cantabrian, Central, Iberian,
25 Pyrenees and Sierra Nevada mountain ranges, respectively). At these colder sites, the melt season
26 occurs mostly in the spring and tends to occur very fast. In contrast, the areas where the melt rates
27 dominated snow cover duration were located systematically at lower elevations, due to the high
28 interannual variability in the occurrence of annual peak SWE (in winter or early spring), yielding
29 highly variable melt rates. However, in colder sites the melt season occurs mostly in spring and it is
30 very fast in most of the years. The results highlight the control that the seasonal precipitation
31 patterns, in combination with temperature, exert on the seasonal snow cover duration by influencing
32 the peak SWE and suggest a future increased importance of melt rates as temperatures increase.
33 Despite the high climatological variability of the Iberian mountain ranges, the results showed a

34 consistent behaviour along the different mountain ranges, indicating that the methods and results
35 may be transferrable to other temperate mountain areas of the world.

36 Keywords: snowpack, mountains, peak SWE, snow cover duration, melt rate

37 **Introduction**

38 Snowpack quantity and snow cover duration determine the annual freshwater budget and its
39 seasonality for mountain regions (Barnett et al., 2005). In addition, snow cover duration directly
40 affects plant and animal phenology, especially the timing and annual magnitude of forest growth, as
41 Sanmiguel-Vallelado et al., (2021) demonstrated in Iberia for the *Pinus uncinata* forests of the
42 Pyrenees. Furthermore, snow dictates the duration and success of winter tourism, which is
43 becoming one of the main sources of income for many mountain regions of the world (Gilaberte-
44 Búrdalo et al., 2017; Steiger et al., 2019).

45 The snowpack over temperate mountain ranges exhibits unique characteristics compared with other
46 mountain areas of the world. Despite the relatively mild winter temperatures, the snowpack tends to
47 be deeper than at higher latitudes; it also exhibits rapid densification, thus being an effective
48 freshwater storage system (Fayad et al., 2017). The snowpack has nearly isothermal conditions for
49 most of the snow season, receiving abundant incoming solar radiation due to the latitude of the
50 temperate mountain ranges (between $\sim 30^\circ$ and $\sim 40^\circ$ in the Northern and Southern Hemispheres),
51 and high sublimation rates (Herrero and Polo, 2016). The snowpack exhibits a high interannual
52 variability, due to spatial differences in precipitation and large elevation gradients (Alonso-
53 González et al., 2020a, 2020b).

54 As a consequence of their lack of cold content and their sensitivity to precipitation-phase
55 partitioning, the snowpacks over temperate mountain ranges are highly vulnerable to the ongoing
56 climate warming (Alonso-González et al., 2020c; Evan and Eisenman, 2021; López-Moreno et al.,
57 2017a; Yilmaz et al., 2019). A major risk of decline in snow cover duration over these temperate
58 regions exists, which endangers the availability of freshwater resources during the long, dry months
59 (García-Ruiz et al., 2011). All these changes are being observed across the Iberian Peninsula, where
60 its mountainous terrain leads to a well-developed seasonal snowpack in various mountain ranges
61 (Cantabrian, Central, Iberian, Pyrenees, and Sierra Nevada mountain ranges) (Alonso-González et
62 al., 2020b). However, the snowpack exhibits high variability in terms of duration and amount,
63 especially at the lower elevations. Such variability is explained by the high climatological diversity

64 of the Iberian mountain ranges and the seasonal synoptic conditions (Alonso-González et al.,
65 2020a).

66 Snowpack magnitude, which is often quantified by the peak snow water equivalent (SWE) or
67 accumulated SWE (Fassnacht and López-Moreno, 2020), strongly controls the amount of water
68 available during the melting period. However, the duration of snow cover dictates many of the
69 biochemical processes controlled by the snowpack, such as soil temperature (Bender et al., 2020;
70 Zhang et al., 2018), microbial activity (Zhang et al., 2014), vegetation growth (Sanmiguel-Vallelado
71 et al., 2019) and animal phenology (Robinson and Merrill, 2012). In addition, the snow cover
72 duration determines the seasonality of different hydrological processes, such as soil moisture
73 (Williams et al., 2009), hydrograph depletion (Julander and Clayton, 2018) and the occurrence of
74 rain-on-snow events (Morán-Tejeda et al., 2016). Snow cover duration can be more accurately
75 derived from remote sensing products (Gascoin et al., 2020) compared to SWE or snow depth that
76 require direct observations or modelling approaches (Painter et al., 2016; Revuelto et al., 2016).
77 Thus, it is important to study the relation between the snow cover and the amount of snow, as it
78 provides an interesting basis for future studies. The duration of the snow cover over the ground at a
79 given location and in a given year depends on the combination of the amount and timing of
80 snowfall and the seasonal melt rate after the occurrence of peak SWE (Harpold et al., 2017). In
81 other words, the duration of the snow cover depends on the maximum amount of snow to be melted
82 and the rate of said melt. The quantification of the contribution of the two factors, namely peak
83 SWE and melt rate, is relevant in understanding the spatiotemporal variability of snow cover
84 duration and, more importantly, to consider how climate change could impact snow cover duration
85 at any given location. Previous research has revealed that the effect of temperature or precipitation
86 on snow cover durations changes over space, with a marked elevational pattern; temperature is the
87 main control at low elevations, whereas the main control in terms of accumulation shifts to
88 precipitation at high elevations (Morán-Tejeda et al., 2013; Sospedra-Alfonso and Merryfield,
89 2017), illustrating the correlation between faster melt rates and lower snow accumulations.
90 However, if snow cover duration mostly depends on accumulated snow, the response of snow cover
91 duration to a climate warming will be strongly influenced by the seasonal timing of the
92 precipitation, the seasonal differences in projected precipitation changes and the timing of peak
93 SWE. Notably, the projected changes in precipitation are highly uncertain in most mountainous
94 areas (Nogués-Bravo et al., 2008). If peak SWE generally occurs at the end of the coldest period of
95 the year, the effect of warmer temperatures might be dampened. Conversely, for locations where
96 peak SWE occurs later in the season because of snowfall during the spring (Caesar et al., 2006),

97 snow cover duration might be strongly affected by higher temperatures since the occurrence of
98 rainfall will be much higher than snowfall (López-Moreno et al., 2020a). In addition, if melt rates
99 dominate snow cover duration, the latter will be controlled more by temperature changes; in this
100 case, melt rates might be less intense as the climate warms due to an earlier occurrence of melting
101 and, thus, less solar loading (Alonso-González et al., 2020c; Musselman et al., 2017; Wu et al.,
102 2018).

103 In the present study, we use a long-term (1980–2014) gridded snow database for the mountains of
104 the Iberian Peninsula (Alonso-González et al., 2018). The Iberian Peninsula exhibits large
105 climatological variability, with its mountain ranges being a good representation of the temperate
106 mountains of the world. To investigate whether seasonal snow cover duration interannual variability
107 is controlled more by the amount of snow accumulation (peak SWE) or by the intensity of the melt
108 rate, we tried to find differences among different-analysed mountain ranges since they exhibit
109 contrasting climatic and snow conditions (Alonso-González et al., 2020b). Such differences may
110 provide useful information to foresee how projected climate change might affect, and with what
111 uncertainty, snow cover duration at different areas of temperate mountain ranges, thereby helping to
112 anticipate the related effects on different environmental and socioeconomic sectors.

113 **Study Area**

114 The Iberian Peninsula is located at the southwestern edge of Europe. Its climatology is strongly
115 influenced by its complex topography and proximity to both the Mediterranean Sea and the Atlantic
116 Ocean, covering a full transition from Mediterranean to Oceanic climates and therefore being one of
117 the areas of Europe with high climatological variability (Peel et al., 2007). Although some locations
118 in Iberia can receive large amounts of annual precipitation, precipitation exhibits high interannual
119 variability and Iberia is generally considered a water-scarce region. Moreover, large areas of the
120 peninsula are highly dependent on water resources from mountain areas and much of this water
121 comes from the snowpack. Total precipitation varies from less than 300 mm yr⁻¹ to more than 1500
122 mm yr⁻¹ and may exceed 2500 mm yr⁻¹ locally in specific locations (Palacios and De Marcos,
123 1998). In the Mediterranean climate, where most precipitation occurs during the winter months
124 (López-Moreno et al., 2011, 2017a), the snowpack becomes critical because it breaks the strong
125 seasonality of the available freshwater resources, resulting in a better synchronization of the water
126 availability with the high demand during the dry and warm season (López-Moreno and García-Ruiz,
127 2004). Atmospheric circulation controls the interannual variability of the precipitation (Trigo et al.,
128 2004). Droughts are frequent and affect the streamflow of the main Iberian basins (Lorenzo-Lacruz

129 et al., 2013). This large precipitation and streamflow variability makes Iberia highly dependent on
130 the water management, and Spain is one of the countries with the most hydrological regulation
131 (Berga-Casafont, 2003).

132 Snow is common over Iberia, including some snowfall events at lower elevations (Aran et al., 2010;
133 Mora et al., 2016). Snowfalls are common every year over wide areas of Iberia due to the presence
134 of a central plateau with an average elevation of 650 m above sea level. In addition, there are five
135 main mountain systems that exceed 2000 m a.s.l. ranging from west to east across Iberia; two of
136 them (Pyrenees and Sierra Nevada) surpass 3000 m a.s.l. (Fig. 1). Mountain ranges exhibit seasonal,
137 long-lasting and deep snowpacks whose characteristics differ due to the climatological
138 particularities of each region (Alonso-González et al., 2020b). Specifically, in Iberia, snow has
139 important implications in different key features of the region, including its hydrology (López-
140 Moreno and García-Ruiz, 2004; Sanmiguel-Vallelado et al., 2017), ecology (Sanmiguel-Vallelado et
141 al., 2021), economy (Lasanta et al., 2007) and risk management (Muntán et al., 2009).

142

143

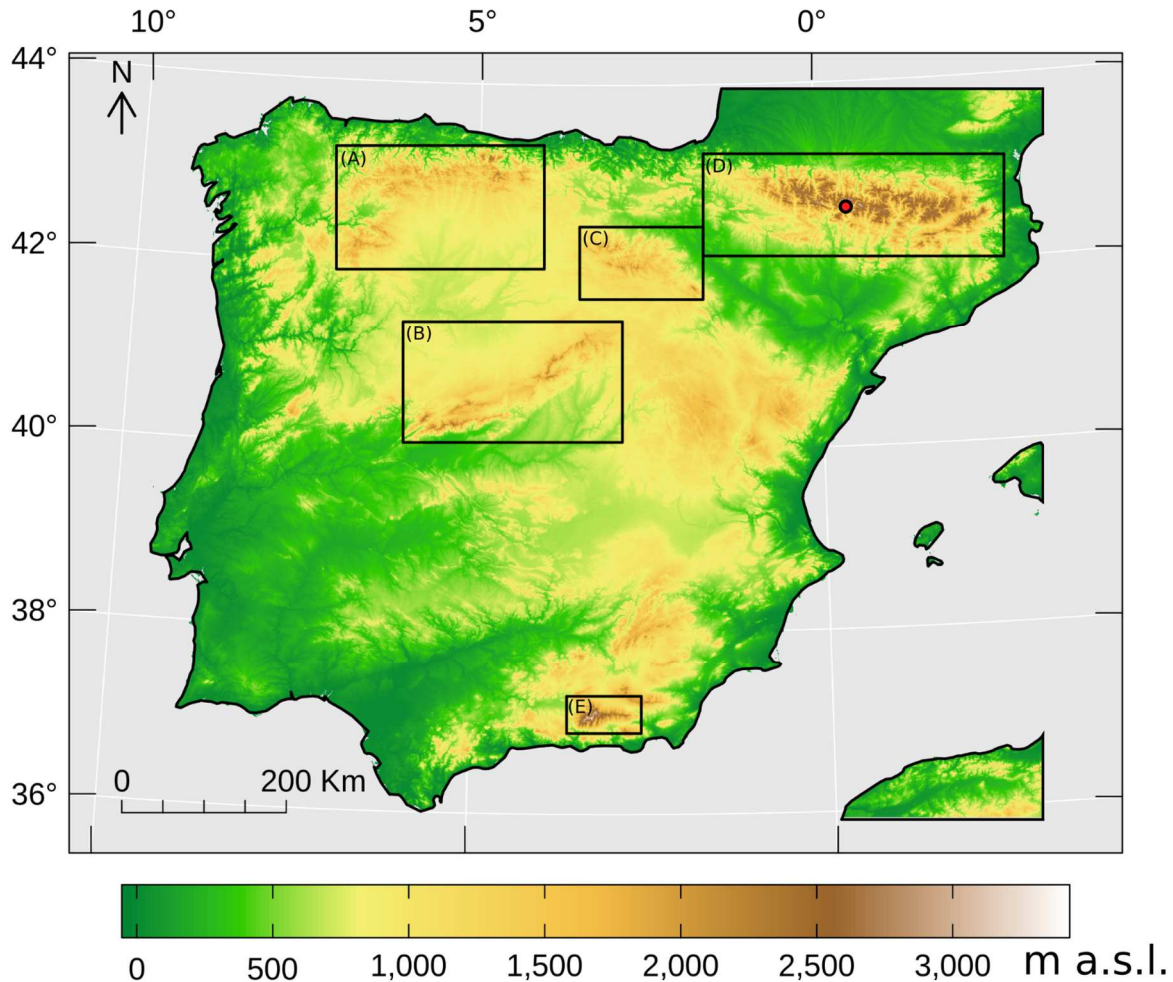


Figure 1: Main mountain ranges of the Iberian Peninsula; A) Cantabrian, B) Central, C) Iberian, D) Pyrenees and E) Sierra Nevada. The red circle indicates the location of the SWE simulated time series shown as an example in this paper.

144

145 Data and Methods

146 We used a daily gridded snowpack database covering the entire Iberian Peninsula for the period
 147 from 1980 to 2014 (Alonso-González et al., 2018). The database was developed using a regional
 148 atmospheric simulation (García-Valdecasas Ojeda et al., 2017) from the Weather Research and
 149 Forecast (WRF) model version 3.8 (Skamarock et al., 2008), at a 10 km spatial resolution as the
 150 meteorological forcing for the Factorial Snow Model (FSM 1.0, Essery, 2015). Given the coarse
 151 spatial resolution (10 km) WRF outputs were corrected from the elevation of the native grid of the
 152 simulation to different elevation bands at 100 m intervals for each simulated grid cell using a
 153 combination of radiative, barometric and psychrometric formulae, as well as lapse-rates. Thus, the
 154 simulated 2 m temperature of the WRF was corrected using the standard air temperature lapse rate
 155 ($\beta = 0.0065 \text{ K m}^{-1}$) and the surface pressure was adjusted using the barometric formula. The long-

156 wave radiation was estimated according to the Stefan–Boltzmann law, using an all-sky conditions
157 parametrization of the emissivity based on the relative humidity (RH) at the elevation of 700 mb to
158 estimate the cloud cover. The RH was projected by correcting the dew-point temperature for the
159 elevation. Both the RH and long-wave-radiation parametrizations have been widely used in the
160 literature and have also been implemented in meteorological distribution models (Liston and Elder,
161 2006). Finally, the precipitation phase partitioning was calculated on the basis of the estimated
162 temperature of the surface of the hydrometeors using the equations proposed by Harder and
163 Pomeroy (2013). A detailed description of the mathematical formulae as well as a graphical scheme
164 can be found in Alonso-González et al. (2018). To disaggregate the semi-distributed fashion (i.e.,
165 elevation bands distribution) of the snowpack database, we interpolated the snowpack series over a
166 DEM of 1km resolution. The distributed snow series over each objective cell of the 1 km DEM was
167 generated by the weighted average of eight neighbour cells in the nearest two elevation bands
168 (directly higher and lower). The distance between each objective cell and four cells in the nearest
169 two elevation bands inside the three-dimensional space of the semi-distributed database was used to
170 generate the new series from the weighted average of the semi-distributed series.

171 Alonso-González et al. (2018) compared the database with both remote sensing imagery and in situ
172 observations of snow height (HS) and SWE and illustrated the database's spatial and temporal
173 consistency. A comparison with MODIS gap-filled snow cover products showed a mean absolute
174 error of 6.07%, and a coefficient of determination (R^2) of 0.76. In addition, the available SWE and
175 HS series for the Iberian Peninsula were used to validate the intra-annual patterns of accumulation
176 at different percentiles, with Cohen's kappa value (k) greater than 0.6. The database has been used
177 for different studies over Iberia, including climatology (Alonso-González et al., 2020b, 2020a),
178 hydrology (Morán-Tejeda et al., 2019) and ecology (Sanmiguel-Vallelado et al., 2019). An example
179 of a time series of SWE for a single cell (red circle in Figure 1) across different elevation bands
180 retrieved from the database is shown in Figure 2.

181

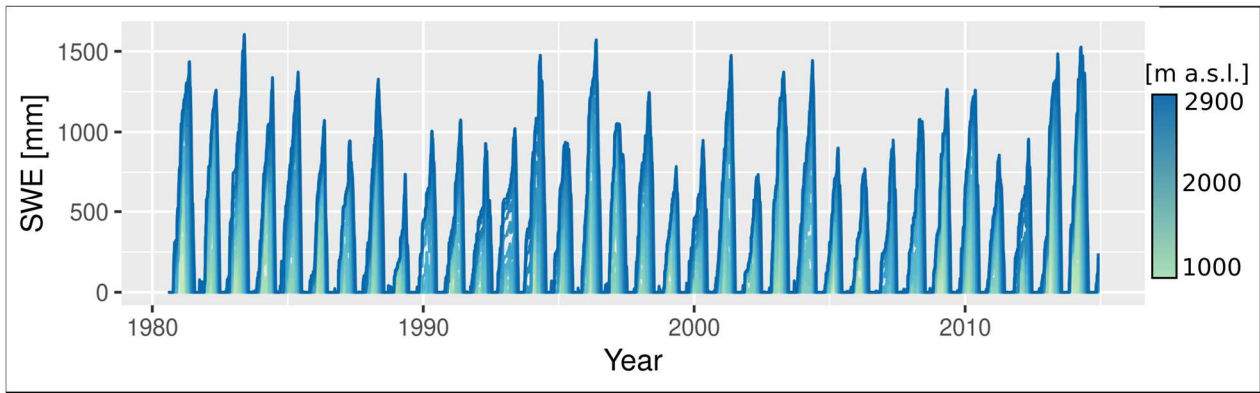


Figure 2: SWE time series retrieved for the Pyrenees from the snowpack database at different elevation bands (represented by the colour palette) covering the whole study period daily.

182

183 To remove ephemeral snowpacks for any year, we only considered snow as seasonal when more
 184 than 30 mm of SWE remained for more than 30 consecutive days. These thresholds were selected
 185 on the basis of Sturm et al. (1995) but were adapted to the study area on the basis of the snow
 186 climatology created by Alonso-González et al. (2020b). This processing was performed for each
 187 season for each cell; cells having less five snow season respecting the above mentioned criteria
 188 (SWE > 30 mm for more than 30 consecutive days) were removed from the analysis. For each
 189 year and for each cell in we calculated the peak SWE [mm], the snow cover duration [days] and the
 190 seasonal melt rate [mm day⁻¹]. The seasonal melt rate was computed in millimetres per day as the
 191 peak SWE divided by the time from the date of peak SWE to the date of the end of the snow season,
 192 or snow disappearance. The duration was defined as the number of days with continuous snow
 193 cover; thus, no early or late season accumulation and complete melt events were considered. In
 194 addition, in the rare case of a complete mid-season melt, the latest snow season was used.

195 To determine the relative influence of the peak SWE and the melt rate (independent variables) to
 196 explain the duration of snow cover (dependent variable) (Figure 3), we used a backward stepwise
 197 linear regression model in the form

$$198 \quad D = \beta_0 + \beta_P * P + \beta_M * M \quad (1),$$

199 where β_0 is the y-intercept; β_P is the coefficient associated with peak SWE, P ; and β_M is the
 200 coefficient associated with the seasonal melt rate, M . Since the regression was stepwise, the best-
 201 fitting independent variable (i.e. either the peak SWE or the melt rate) was chosen first. Iteratively,
 202 each variable was considered for removal/addition on the basis of the variations of the Akaike
 203 information criterion (AIC). The coefficients were then standardized by multiplying the regression-
 204 based coefficient by the ratio of the standard deviation of the dependent variable (D) by the standard
 205 deviation of the independent variable (P or M), providing a simple quantification of the weight of

206 each independent variable on the duration of snow cover. We then evaluated how β_P and β_M were
 207 distributed along the elevations in the main mountain ranges of Iberia. We then extracted the
 208 elevation values of the DEM using the β_P and β_M values, to evaluate the β -coefficients variation with
 209 the elevation. Thus, we studied the elevations where one of the β -coefficients was greater than the
 210 other, or only one variable was selected by the stepwise approach . All the calculations were
 211 performed using the R programming language (R Core Team, 2020) at the supercomputing facilities
 212 of the Spanish Research Council. We use one location in the Pyrenees as an example (the same
 213 location indicated in Figure 2) to illustrate the specific results and then provide the results of the
 214 distributed analyses over the Iberian mountains.

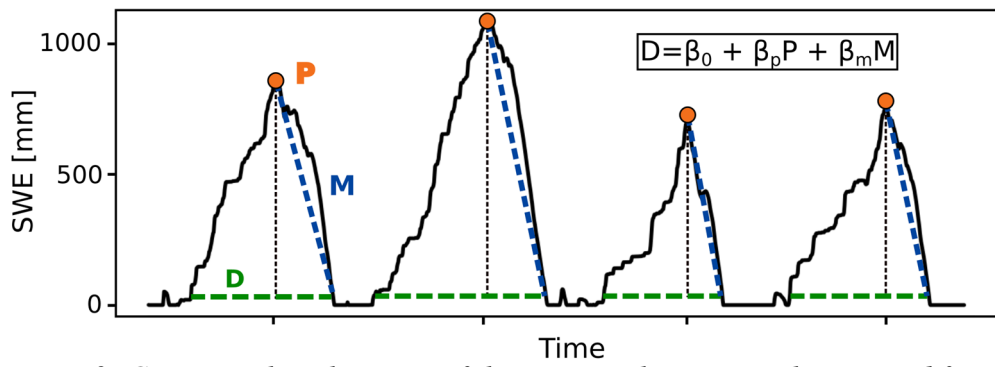


Figure 3: Conceptual explanation of the stepwise linear correlation used for all the cells of the snowpack database. The snowpack duration (D) is modelled from the peak SWE (P) and the seasonal melt rate (M) for each cell of the snowpack database.

215

216 Results and Discussion

217

218 The main temporal patterns and the relationship with elevation of the three snow indexes (fig. 4)
 219 can be exemplified by a single cell of the Pyrenees (red dot in Figure 1). Peak SWE exhibits
 220 noticeable temporal variability at all elevations but with a decrease with increasing elevation
 221 (coefficient of variation (CV) of 0.48, 0.30 and 0.23 at 2000, 2400 and 2900 m a.s.l., respectively).
 222 This result is mainly attributed to the snowpacks in temperate regions being consistently close to the
 223 zero degree isotherm since they are highly sensitive to the precipitation partition phase (Fayad and
 224 Gascoin, 2020). Thus, the elevation ensures colder temperatures and more constant peak SWE

values, which are mostly regulated by the precipitation, which is why several studies have found the higher areas (or colder locations) of mountain ranges to be less affected by climate warming worldwide (Alonso-González et al., 2020c; Marty et al., 2017; Matiu et al., 2021; Pierce and Cayan, 2013; Sproles et al., 2013). As in the case of peak SWE, an obvious relation exists between the duration of the snow cover and the elevation, with longer durations at higher elevations (Figure 4); the interannual variability of the snow cover duration also decreases with increasing elevation (CV of 0.33, 0.11 and 0.09 at 2000, 2400 and 2900 m a.s.l., respectively, in this particular example). The melt rates showed a more complex spatial and temporal behaviour. The lower CV for the snow cover duration compared with that for the peak SWE might explain the inversions in the relation of the melt rates with the elevation in some particular years. The seasons with thicker (shallower) snowpacks do not increase (decrease) linearly with the snow cover duration since the melt rates show different values as the snow season progresses. On average, the melt rates tend to increase with increasing elevation (average of 14.1, 19.5 and 19.0 mm day⁻¹ at 2000, 2400 and 2900 m a.s.l., respectively, in this particular example); however, this relation is not as clear as that observed for the peak SWE and the snow cover duration. This pattern occurs because an effective melt not only requires temperature warmer than 0°C but also a considerable increase in incoming solar radiation and decreased albedo at the end of the winter (Musselman et al., 2017).

242

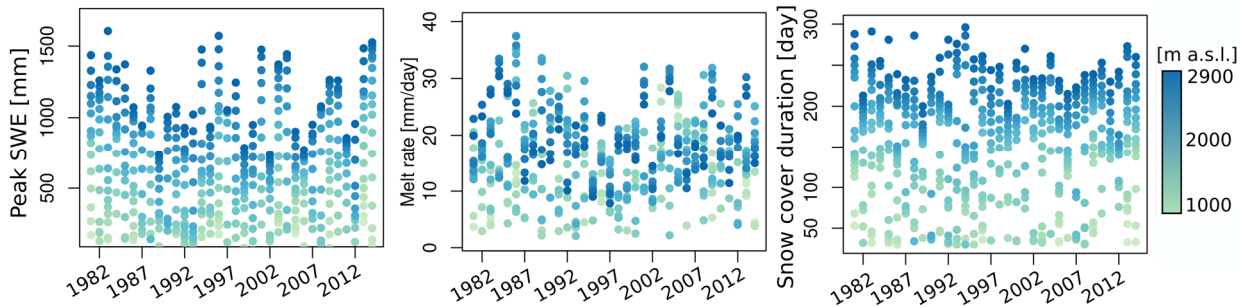


Figure 4: Peak SWE (left), melt rate (middle) and snow season duration (right) at different elevations (represented by the colour palette), as derived from the single-cell snow series in Figure 2.

243

At the sample location in the Pyrenees (Figures 1 and 4), the β -coefficients of the peak SWE and melt rate as well as the adjusted R^2 of the stepwise regression model are correlated with the elevation (Figure 5), most likely due to local particularities of this specific location. The peak SWE exhibited a higher β -coefficient than the melt rates at all elevation bands. At the 1400–1800 and 2400–2900 m elevation bands, the melt rate was not even included in the model by the stepwise

algorithm as a predictor variable. Thus, the model suggests that, for this single cell example (Figure 4), the peak SWE exerts greater control of the snow cover duration than the melt rates. Here, the maximum explained variance of the model is found at low and medium elevations and the overall evolution of adjusted- R^2 follows the evolution of the β -coefficients of peak SWE, with a negligible effect when the melt rate is also included in the model as a predictor variable.

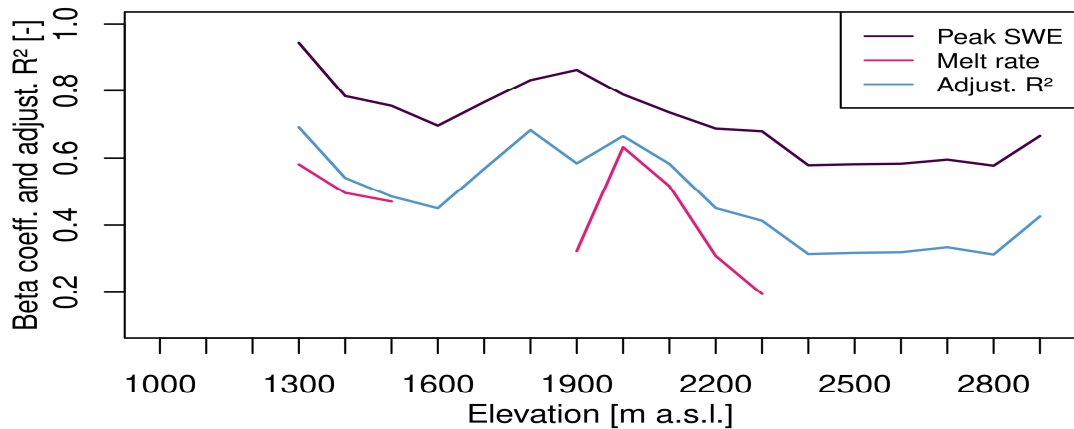


Figure 5: Adjusted R^2 and β -coefficients of the model's results for a single cell (the one used as an example in Figs. 2 and 4) at different elevations.

We extended the previously methodology described for a single cell (Figure 5) to the all study area. A large spatial variability is observed in the peak SWE, melt rate and the snow cover duration over Iberia (Figure 6), with strong differences also observed within the same mountain ranges, even at similar elevations, as reported in previous studies(Alonso-González et al., 2020b). Among the five main mountain ranges of Iberia, the Pyrenees and Cantabrian mountains receive the most snow, with a maximum SWE approaching 2000 mm and a snow cover duration as long as 290 days in the most favourable locations (Figure 6). By contrast, the Sierra Nevada exhibited lower values when similar elevation bands were compared. A complete description of the snow climatology and the differences between mountain ranges can be found in the work of Alonso-González et al. (2020b).

As expected, the snow season duration and peak SWE are mostly controlled by elevation. In addition, melt rates tend to be faster at the higher elevations (Figure 6), consistent with other studies that found faster melt rates occurring later in the snow season under conditions of greater incoming radiation (Musselman et al., 2017; Wu et al.,2018). Peak SWE is more variable at lower than at higher elevation, leading to very different melt-rates having a significant influence on the snow

269 cover duration. The interannual CV estimated for the snow cover duration and peak SWE follows a
270 similar spatial pattern, with a clear decrease with increasing elevation (Figure 6). This effect might
271 be a consequence of the low values of each index (low elevations) that can lead to extremely large
272 CV values; however, the preprocessing of the snow series where each snow season must meet the
273 minimum accumulation and duration criteria prevents the standard deviation from being divided by
274 small mean values. Differences in CV values were observed between the three snow indexes. The
275 CV values for the mean season duration were lower than for the peak SWE, whose CV values were,
276 in turn, lower than those for the melt rates.

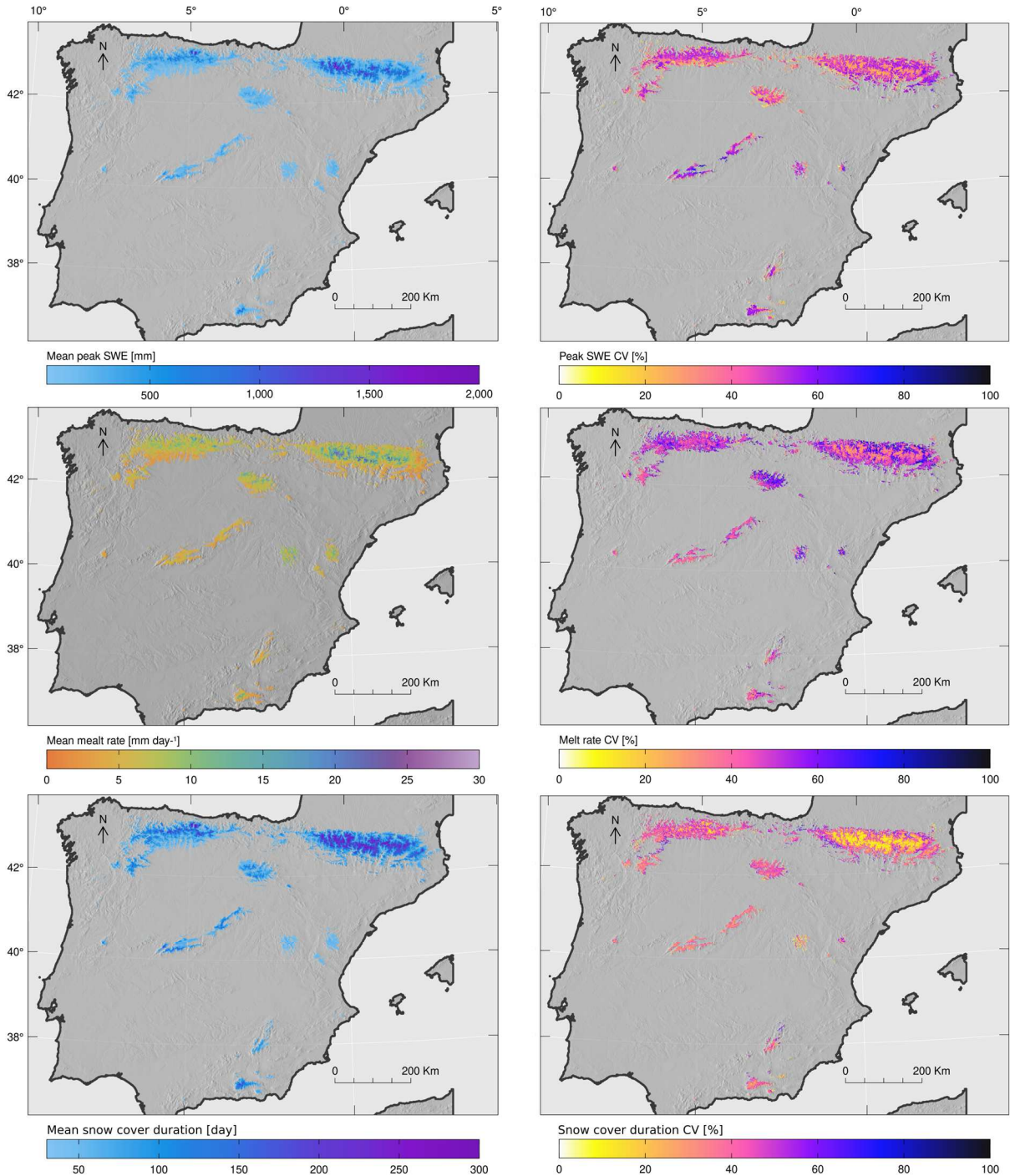


Figure 6: Mean peak SWE and its CV (upper panels), melt rate and its CV (middle panels), and snow season duration and its CV (bottom panels) in the Iberian peninsula.

277

278 The stepwise models used to predict the snow cover duration from the peak SWE and the melt rate
 279 showed an average coefficient of determination (R^2 -adjust) of 0.5. The adjusted R^2 values of the
 280 models showed no clear dependence on the elevation or differences between mountain ranges,
 281 although the highest determination coefficients were found in the band between 1500 and 2000 m
 282 a.s.l. and the variability of the adjusted R^2 values tended to decrease with increasing elevation

283 (Supplementary Figure 1). This greater variability at the lower elevations was likely caused by the
284 fact that there were more cases at the lower elevations, in addition to a higher variability in the
285 snow indexes.

286 Focusing on the Pyrenees, modelling results showed that snow cover duration is more sensitive to
287 peal SWE than to melt rates (Figure 7). The peak SWE was excluded by the stepwise approach
288 (Figure 7 left panel) in only 2.4% of the cells. Moreover, considering the subset of cells where
289 either peak swe and melt rate (P&M) or only melt rate (M) were selected by the stepwise model,
290 melt rate β -coefficients were higher than peak swe one in only 6.8% of the cases" (Figure 7 right
291 panel). By contrast, the cases where the model considered only the peak SWE represented 35.6% of
292 cells (Figure 7a), increasing to 93.2% of cells when both indexes were included and the peak SWE
293 exhibited higher β -coefficients (Figure 7 right panel).In addition, the cells where the melt rates
294 exhibited a higher influence were concentrated at the lower elevations, with an average elevation of
295 1180 m a.s.l., in contrast with the 1740 m a.s.l. elevation in the cells where the peak SWE exhibited
296 a higher β -coefficient (Figure 7 right panel). Surprisingly, despite the strongly contrasting
297 climatological characteristics of the five Iberian mountain ranges (Alonso-González et al., 2020b),
298 this spatial pattern of the β -coefficient of the peak SWE (β -P) and melt rate (β -M) is similar over the
299 other Iberian mountain ranges (Table 1 and Supplementary Figure 2). Slight differences are
300 observed in the average elevation values as a consequence of the different hypsography of each
301 range (Table 1). This finding is consistent with the results of similar studies developed in the
302 western United States (Trujillo and Molotch, 2014), where deeper snowpacks lead to longer snow
303 seasons and higher melt rates. Thus, the relative areas where the β -M is higher than the β -P decrease
304 regularly from the lower (Iberian, Central and Cantabrian ranges with 81.6%, 89.2% and 89.1%,
305 respectively) to the higher (Pyrenees and Sierra Nevada with 93.2% and 95.5%, respectively)
306 elevation mountain ranges. Independently from the elevation, the accumulation (i.e. peak SWE)
307 dominates the snow cover duration. However, at the lower areas the melt rates increase its
308 [importance](#) in controlling the snow cover duration. This result is particularly relevant, as the Iberian
309 snowpacks have shown contrasting behaviours due to the climatological variability of the Iberian
310 Peninsula (Alonso-González et al., 2020b). Thus, this finding suggests that the results of the present
311 study could be extrapolated to other regions of the planet at comparable latitudes where the peak
312 SWE is reached with a low cold content because the pattern remains similar over the different
313 mountain ranges. However, snowpacks over high-latitude sites may present different behaviours
314 because of different partitioning of the energy and mass balance of the snowpacks, including a

315 completely different seasonal distribution of the incoming solar radiation combined with (in
 316 general) a shallower snowpack.

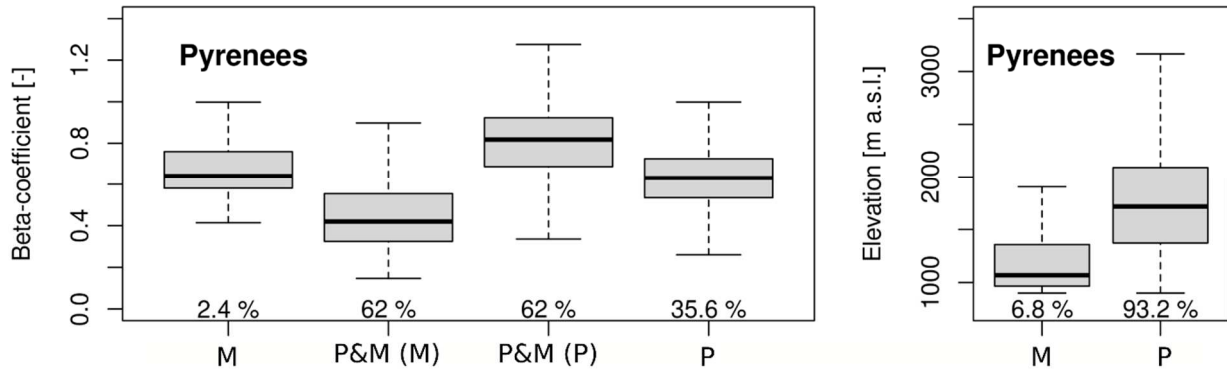


Figure 7: β -Coefficients for the peak SWE and the melt rate (left panel) for different model configurations, and the altitudinal distribution of the β -coefficients in the Pyrenees (right panel). M indicates model configurations when only melt rate is selected (2.4% of cells), P indicates model configurations when only peak SWE is selected (35.6%) and P&M indicates model configurations when both predictors are included (62%). The distribution of the β -coefficients with the elevations indicates the elevations where one of the predictors showed a higher β -coefficient; (left boxplot) altitudinal distribution of the cells where melt rate β -Coefficients > peak swe β -Coefficients, including M and P&M models; (right boxplot) altitudinal distribution of the cells where peak swe β -Coefficients > melt rate β -Coefficients including P and P&M models. The percentages showed in both panels are the relative are of the range where it is possible to find its correspondent model.

317

318

Table 1: Averaged β -coefficients for the peak SWE and the melt rate and the average elevation of the cells where higher peak SWE or melt rate β -coefficient were found.

Ranges	Melt rate		Melt rate and Peak SWE				Peak SWE		Elevation		Elevation	
	β_m (β_p is 0)	%	β_m	β_p	%	β_p	%	m	%	m	%	
Cantabrian	0.70	2.4	0.65	1.00	62.0	0.73	35.5	1230	10.9	1470	89.1	
Central	0.72	5.5	0.54	0.91	41.9	0.70	52.6	1520	10.8	1727	89.2	
Iberian	0.67	4.6	0.60	0.90	84.4	0.75	11.0	1312	18.4	1517	81.6	

Pyrenees	0.67	2.4	0.47	0.82	62.0	0.63	35.6	1180	6.8	1740	93.2
S. Nevada	0.71	1.2	0.45	0.91	50.8	0.74	48.0	1892	4.2	2187	95.8

319
320 The greater dependency of the snow season duration on the peak SWE than on the melt rate (Table
321 1) indicates that the precipitation is a mayor driver of the snow season duration. As despite the
322 whole energy balance has its own influence, the peak SWE is mostly controlled by precipitation,
323 especially at the higher elevations (Morán-Tejeda et al., 2013; Musselman et al., 2021). At high
324 elevation, snow melts late in spring and the depletion curve rather steep as consequence of the rise
325 of shortwave radiation; at lower elevations, melting occurs earlier and is a function of the date of
326 peak SWE. Thus, the melt rates in the areas where the peak SWE occurs earlier tends to be more
327 variable than in the areas where the peak SWE occurs latter (i.e. the higher and colder areas).

328 Despite most atmospheric models showing a high consensus to project a generalized warming, the
329 climate change projections show large disagreements and uncertainties about how the precipitation
330 could evolve in the next decades (Kharin et al., 2013). In addition, the sensitivity to warming of the
331 snow accumulation may be different, even in areas with comparable climatological characteristics
332 due to local effects (López-Moreno et al., 2017a). The seasonal precipitation patterns will play a
333 key role, as the peak SWE is affected by the winter and spring precipitation and the surface
334 temperatures of the Iberian Peninsula are expected to increase similarly for the winter and spring
335 seasons (Carvalho et al., 2020). Lorenzo and Alvarez (2020) have reported differences in the future
336 seasonal precipitation patterns of Iberia estimated from high-resolution atmospheric simulations
337 extracted from the EURO-CORDEX project. Their results highlight the uncertainty of the
338 projections to simulate the future evolution of the precipitation and the spatial variability of the
339 accumulated precipitation changes. Nevertheless, they show a general increase in the total winter
340 precipitation of approximately 15%, with a decrease as large as 20% in the spring total
341 precipitation. These results suggest that the areas where the peak SWE is controlled by the total
342 winter precipitation (warmer areas) will exhibit a different evolution than those controlled by the
343 spring precipitation (colder areas). However, even under scenarios of substantial precipitation
344 increases, the sensitivity of the peak SWE has proven to be negative in Iberia under warmer
345 conditions (Alonso-González et al., 2020c), including in the higher elevations or colder areas. These
346 results are consistent with a sensitivity analysis performed for most of the mountain climates of the
347 world (López-Moreno et al., 2020a), where consistent projected climate warming led to a decrease
348 in both the peak SWE and the snow cover duration in most of the mountains of the planet. Thus, a
349 generalized decrease in the length of the snow seasons is expected on the basis of the decline of the

350 peak SWE as a consequence of warming, providing continuity with the reported ongoing trend
351 estimated from long-term reanalysis simulations in the Pyrenees (López-Moreno et al., 2020b).

352 The results presented here suggest that the areas where the melt rates play a key role in controlling
353 the snow seasonal duration are located at the lower elevations. These results are consistent for the
354 different mountain ranges despite their climatological differences. The average elevations where the
355 melt rates' dependency dominates the peak SWE dependency were similar in all the investigated
356 mountain ranges, with larger differences in the Pyrenees. This effect is caused by the hypsometry of
357 each mountain ranges. In most of the areas, the duration of the snow cover is controlled by the peak
358 SWE, making the average elevation between both cases similar, as there are many more areas at
359 low elevations than at high elevations. The slight differences between mountain ranges in the
360 percentage of area where the melt rates exert greater control of the snow season duration can be
361 easily explained by the differences in the hypsography of the mountain ranges (i.e. a higher
362 percentage of the total area is at a low elevation). This difference in hypsography likely explains
363 why the Pyrenees and Sierra Nevada exhibit a higher percentage of their area where the snow cover
364 seasonal duration is controlled by the peak SWE (93.2% and 95.5%, respectively), as they have the
365 higher elevational ranges among the Iberian mountain ranges. Our results may indicate that the
366 control exerted by the melt rates over the snow cover seasonal duration could increase in the future
367 because of the rise of the winter zero-degree isotherm. This finding is relevant, as previous studies
368 have reported a generalized negative sensitivity of the melt rates to warming (Alonso-González et
369 al., 2020c; Musselman et al., 2017). However, despite the lower melt rates, a generalized decrease
370 in the snow cover duration as a consequence of the lower peak SWE values is expected. The lower
371 melt rates will not compensate for lower peak SWE values, as they are the result of a different level
372 of decrease in the peak SWE and the snow season length. The available projections for precipitation
373 and temperature show different seasonal patterns in their expected future evolution and different
374 increases in the role of the melt rate at the lower elevations. The snow cover duration at high
375 elevations (greater than 2000–2200 m a.s.l.) could be more strongly influenced by climate change
376 than those at medium and low elevations a result already observed in the Pyrenees over the last
377 decades (López-Moreno et al., 2020b).

378 Despite the relatively high R^2 adjusted values found in the models (Supplementary Figure 1), there
379 is an important part of the variance that it is unexplained by the models. It is obvious that other
380 factors different form the melt rates and the peak SWE could condition the duration of the snow
381 cover. For example, some winters may influence the shape of the daily snowpack time series,
382 introducing some uncertainties in the models; specifically the accumulation and melt are often not

383 linear (Figure 3). It is possible to find some seasons where exceptionally dry periods followed by an
384 intense precipitation period lead to a secondary but relevant peak SWE during the spring. These
385 situations may delay the melt out day, increasing the impact on the length of the snow season
386 duration. In addition, it may be possible to find seasons where the exact day of occurrence of the
387 peak SWE could be difficult to identify because numerous days have the same SWE peak. This
388 could have some influence in the estimation of the melt rates in those seasons. However, these
389 situations are rare, due to the regional nature of the timeseries of the snowpack database. Thus,
390 despite the uncertainties, the results of the present study are easy to generalize, being transferrable
391 to other temperate climate mountain ranges of the world. The results presented here cannot be
392 extrapolated to small spatial scales where the local climatology characteristics explain an important
393 part of the spatial variability of the snowpack (López-Moreno et al., 2017b; Revuelto et al., 2020;
394 Fassnacht, 2021). Such an effect is relevant even under warmer conditions, where slope and aspect
395 could lead to more spatially variable snowpacks (López-Moreno et al., 2013) because of the control
396 of the topography over the radiative surface fluxes, accumulation patterns and wind redistribution.
397 In addition, the correlation between melt-rates and peak SWE might be different at the wind
398 redistribution scales due to the local interactions with vegetation and landscape (Pomeroy et al.,
399 2004).

400 **Conclusions**

401 We analysed the roles of the peak SWE and melt rates to explain the temporal and spatial variability
402 of snow cover duration. We used a daily gridded snowpack database derived from numerical
403 simulations; this database has proven to be consistent with both in situ measurements and remote
404 sensing snow cover products. The long-term average and the interannual variability exhibited by the
405 peak SWE, melt rate and snow cover duration highlight the varied conditions of the snowpack
406 existing across the Iberian Peninsula, giving the results of the present study a wider geographical
407 entity, as this snowpack is representative of many other snowpacks over temperate mountain ranges.
408 Using the combination of peak SWE and melt rates to explain the snow cover duration resulted in,
409 on average, an adjusted R^2 of 0.5. We did not find a clear relation between different levels of
410 explained variance with the geographical location, mountain range or elevation range. We found
411 that, in most of the areas of the main mountain ranges of Iberia (~90% of the total area), the peak
412 SWE exerts greater control than the melt rates to explain the interannual variability of the snow
413 cover duration. The areas where the melt rates exerted greater control of the snow season duration
414 were located at lower elevations.

415 Given the key role of the total precipitation in controlling the interannual variability of the peak
416 SWE, the results presented here indicate notable uncertainty in the projections for the future
417 evolution of the snow cover duration. The snow cover duration in colder areas—mostly at higher
418 elevations, where the spring precipitations control much of the seasonal peak SWE—might be
419 particularly uncertain compared with that in warmer areas, where the peak SWE is controlled by the
420 wintertime accumulated precipitation. Nonetheless, the confidence of climate projections toward a
421 warmer climate will lead to a clear generalized decrease of snow cover duration in all mountains of
422 Iberia and most of the mountains of the world. Snow cover duration could be particularly reduced at
423 mid and high elevations. The role of melt rates in controlling the snow seasonal duration may gain
424 importance in the next few decades as a consequence of the rise of the winter zero-degree isotherm.

425

426 **Acknowledgements**

427 This study was supported by the projects: CGL2017-82216-R (HIDROIBERNIEVE) funded by the
428 Spanish Ministry of Economy and Competitiveness, and OPCC-ADAPYR (POCTEFA 2014-2020,
429 Interreg V-A).

430

431 **References**

432 Alonso-González, E., Ignacio López-Moreno, J., Gascoin, S., García-Valdecasas Ojeda, M.,
433 Sanmiguel-Vallelado, A., Navarro-Serrano, F., Revuelto, J., Ceballos, A., Esteban-Parra, M. J. and
434 Essery, R.: Daily gridded datasets of snow depth and snow water equivalent for the Iberian
435 Peninsula from 1980 to 2014, *Earth Syst. Sci. Data*, 10(1), 303–315, doi:10.5194/essd-10-303-2018,
436 2018.

437 Alonso-González, E., López-Moreno, J. I., Navarro-Serrano, F. M. and Revuelto, J.: Impact of
438 North Atlantic Oscillation on the snowpack in Iberian Peninsula mountains, *Water* (Switzerland),
439 12(1), 105, doi:10.3390/w12010105, 2020a.

440 Alonso-González, E., López-Moreno, J. I., Navarro-Serrano, F., Sanmiguel-Vallelado, A., Revuelto,
441 J., Domínguez-Castro, F. and Ceballos, A.: Snow climatology for the mountains in the Iberian
442 Peninsula using satellite imagery and simulations with dynamically downscaled reanalysis data, *Int.*
443 *J. Climatol.*, 40(1), 477–491, doi:10.1002/joc.6223, 2020b.

444 Alonso-González, E., López-Moreno, J. I., Navarro-Serrano, F., Sanmiguel-Vallelado, A., Aznárez-
445 Balta, M., Revuelto, J. and Ceballos, A.: Snowpack sensitivity to temperature, precipitation, and
446 solar radiation variability over an elevational gradient in the Iberian mountains, *Atmos. Res.*, 243,
447 104973, doi:10.1016/j.atmosres.2020.104973, 2020c.

448 Aran, M., Rigo, T. and Bech, J.: Analysis of the hazardous low-altitude snowfall, 8th March 2010,
449 in Catalonia, ... Sept. 1-4, 2010 ..., 12(September), 2010 [online] Available from:
450 <http://adsabs.harvard.edu/abs/2010pcms.confE..77A> (Accessed 28 November 2017), 2010.

451 Barnett, T. P., Adam, J. C. and Lettenmaier, D. P.: Potential impacts of a warming climate on water
452 availability in snow-dominated regions, *Nature*, 438(7066), 303–309, doi:10.1038/nature04141,
453 2005.

454 Bender, E., Lehning, M. and Fiddes, J.: Changes in Climatology, Snow Cover, and Ground
455 Temperatures at High Alpine Locations, *Front. Earth Sci.*, 8, 100, doi:10.3389/feart.2020.00100,
456 2020.

457 Berga-Casafont, L.: Presas y embalses en la España del siglo XX, *Rev. Obras Públicas* , 3438, 37–
458 40 [online] Available from: <https://dialnet.unirioja.es/servlet/articulo?codigo=781617> (Accessed 23
459 November 2020), 2003.

460 Caesar, J., Alexander, L. and Vose, R.: Large-scale changes in observe daily maximum and
461 minimum temperatures: Creation and analysis of a new gridded data set, *J. Geophys. Res. Atmos.*,
462 111(5), doi:10.1029/2005JD006280, 2006.

463 Carvalho, D., Cardoso Pereira, S. and Rocha, A.: Future surface temperature changes for the Iberian
464 Peninsula according to EURO-CORDEX climate projections, *Clim. Dyn.*, 56(1), 123–138,
465 doi:10.1007/s00382-020-05472-3, 2020.

466 Essery, R.: A factorial snowpack model (FSM 1.0), *Geosci. Model Dev.*, 8(12), 3867–3876,
467 doi:10.5194/gmd-8-3867-2015, 2015.

468 Evan, A. and Eisenman, I.: A mechanism for regional variations in snowpack melt under rising
469 temperature, *Nat. Clim. Chang.*, doi:10.1038/s41558-021-00996-w, 2021.

470 Fassnacht, S. R. and López-Moreno, J. I.: Patterns of trends in niveograph characteristics across the
471 western United States from snow telemetry data, *Front. Earth Sci.*, 14(2), 315–325,
472 doi:10.1007/s11707-020-0813-5, 2020.

473 Fassnacht, S.R.: A Call to: More Snow Sampling, *Geoscience*, accepted 18 October 2021.

474 Fayad, A. and Gascoin, S.: The role of liquid water percolation representation in estimating snow
475 water equivalent in a Mediterranean mountain region (Mount Lebanon), *Hydrol. Earth Syst. Sci.*,
476 24(3), 1527–1542, doi:10.5194/hess-24-1527-2020, 2020.

477 Fayad, A., Gascoin, S., Faour, G., López-Moreno, J. I., Drapeau, L., Page, M. Le and Escadafal, R.:
478 Snow hydrology in Mediterranean mountain regions: A review, *J. Hydrol.*, 551, 374–396,
479 doi:10.1016/j.jhydrol.2017.05.063, 2017.

480 García-Ruiz, J. M., López-Moreno, I. I., Vicente-Serrano, S. M., Lasanta-Martínez, T. and Beguería,
481 S.: Mediterranean water resources in a global change scenario, *Earth-Science Rev.*, 105(3–4), 121–
482 139, doi:10.1016/j.earscirev.2011.01.006, 2011.

483 García-Valdecasas Ojeda, M., Gámiz-Fortis, S. R., Castro-Díez, Y. and Esteban-Parra, M. J.:
484 Evaluation of WRF capability to detect dry and wet periods in Spain using drought indices, *J.*
485 *Geophys. Res.*, 122(3), 1569–1594, doi:10.1002/2016JD025683, 2017.

486 Gascoin, S., Dumont, Z. B., Deschamps-Berger, C., Marti, F., Salgues, G., López-Moreno, J. I.,
487 Revuelto, J., Michon, T., Schattan, P. and Hagolle, O.: Estimating fractional snow cover in open
488 terrain from Sentinel-2 using the normalized difference snow index, *Remote Sens.*, 12(18),
489 doi:10.3390/RS12182904, 2020.

490 Gilaberte-Búrdalo, M., López-Moreno, J. I., Morán-Tejeda, E., Jerez, S., Alonso-González, E.,
491 López-Martín, F. and Pino-Otín, M. R.: Assessment of ski condition reliability in the Spanish and
492 Andorran Pyrenees for the second half of the 20th century, *Appl. Geogr.*, 79, 127–142,
493 doi:10.1016/j.apgeog.2016.12.013, 2017.

494 Harder, P. and Pomeroy, J.: Estimating precipitation phase using a psychrometric energy balance
495 method, *Hydrol. Process.*, 27(13), 1901–1914, doi:10.1002/hyp.9799, 2013.

496 Harpold, A. A., Dettinger, M. and Rajagopal, S.: Defining snow drought and why it matters, *Eos*
497 (United States), 98(5), 15–17, doi:10.1029/2017eo068775, 2017.

498 Herrero, J. and Polo, M. J.: Evaposublimation from the snow in the Mediterranean mountains of
499 Sierra Nevada (Spain), *Cryosphere*, 10(6), 2981–2998, doi:10.5194/tc-10-2981-2016, 2016.

500 Julander, R. P. and Clayton, J. A.: Determining the proportion of streamflow that is generated by
501 cold season processes versus summer rainfall in Utah, USA, *J. Hydrol. Reg. Stud.*, 17, 36–46,
502 doi:10.1016/j.ejrh.2018.04.005, 2018.

503 Kharin, V. V., Zwiers, F. W., Zhang, X. and Wehner, M.: Changes in temperature and precipitation
504 extremes in the CMIP5 ensemble, *Clim. Change*, 119(2), 345–357, doi:10.1007/s10584-013-0705-
505 8, 2013.

506 Lasanta, T., Laguna, M. and Vicente-Serrano, S. M.: Do tourism-based ski resorts contribute to the
507 homogeneous development of the Mediterranean mountains? A case study in the Central Spanish
508 Pyrenees, *Tour. Manag.*, 28(5), 1326–1339, doi:10.1016/j.tourman.2007.01.003, 2007.

509 Liston, G. E. and Elder, K.: A meteorological distribution system for high-resolution terrestrial
510 modeling (MicroMet), *J. Hydrometeorol.*, 7(2), 217–234, doi:10.1175/JHM486.1, 2006.

511 López-Moreno, J. I. and García-Ruiz, J. M.: Influence of snow accumulation and snowmelt on
512 streamflow in the central Spanish Pyrenees / Influence de l'accumulation et de la fonte de la neige
513 sur les écoulements dans les Pyrénées centrales espagnoles, *Hydrol. Sci. J.*, 49(5),
514 doi:10.1623/hysj.49.5.787.55135, 2004.

515 López-Moreno, J. I., Vicente-Serrano, S. M., Morán-Tejeda, E., Lorenzo-Lacruz, J., Kenawy, A. and
516 Beniston, M.: Effects of the North Atlantic Oscillation (NAO) on combined temperature and
517 precipitation winter modes in the Mediterranean mountains: Observed relationships and projections
518 for the 21st century, *Glob. Planet. Change*, 77(1–2), 62–76, doi:10.1016/j.gloplacha.2011.03.003,
519 2011.

520 López-Moreno, J. I., Revuelto, J., Gilaberte, M., Morán-Tejeda, E., Pons, M., Jover, E., Esteban, P.,
521 García, C. and Pomeroy, J. W.: The effect of slope aspect on the response of snowpack to climate
522 warming in the Pyrenees, *Theor. Appl. Climatol.*, 117(1), 207–219, doi:10.1007/s00704-013-0991-
523 0, 2013.

524 López-Moreno, J. I., Gascoin, S., Herrero, J., Sproles, E. A., Pons, M., Alonso-González, E.,
525 Hanich, L., Boudhar, A., Musselman, K. N., Molotch, N. P., Sickman, J. and Pomeroy, J.: Different
526 sensitivities of snowpacks to warming in Mediterranean climate mountain areas, *Environ. Res.*
527 *Lett.*, 12(7), doi:10.1088/1748-9326/aa70cb, 2017a.

528 López-Moreno, J. I., Revuelto, J., Alonso-González, E., Sanmiguel-Vallelado, A., Fassnacht, S. R.,
529 Deems, J. and Morán-Tejeda, E.: Using very long-range terrestrial laser scanner to analyze the
530 temporal consistency of the snowpack distribution in a high mountain environment, *J. Mt. Sci.*,
531 14(5), 823–842, doi:10.1007/s11629-016-4086-0, 2017b.

532

533 López-Moreno, J. I., Soubeyroux, J. M., Gascoin, S., Alonso-Gonzalez, E., Durán-Gómez, N.,
534 Lafaysse, M., Vernay, M., Carmagnola, C. and Morin, S.: Long-term trends (1958–2017) in snow
535 cover duration and depth in the Pyrenees, *Int. J. Climatol.*, joc.6571, doi:10.1002/joc.6571, 2020b.

536 Lorenzo-Lacruz, J., Vicente-Serrano, S. M., González-Hidalgo, J. C., López-Moreno, J. I. and
537 Cortesi, N.: Hydrological drought response to meteorological drought in the Iberian Peninsula,
538 *Clim. Res.*, 58(2), 117–131, doi:10.3354/cr01177, 2013.

539 Lorenzo, M. N. and Alvarez, I.: Climate change patterns in precipitation over Spain using
540 CORDEX projections for 2021–2050, *Sci. Total Environ.*, 723, 138024,
541 doi:10.1016/j.scitotenv.2020.138024, 2020.

542 Marty, C., Schlägl, S., Bavay, M. and Lehning, M.: How much can we save? Impact of different
543 emission scenarios on future snow cover in the Alps, *Cryosphere*, 11(1), 517–529, doi:10.5194/tc-
544 11-517-2017, 2017.

545 Matiu, M., Crespi, A., Bertoldi, G., Maria Carmagnola, C., Marty, C., Morin, S., Schöner, W., Cat
546 Berro, D., Chiogna, G., De Gregorio, L., Kotlarski, S., Majone, B., Resch, G., Terzago, S., Valt, M.,
547 Beozzo, W., Cianfarra, P., Gouttevin, I., Marcolini, G., Notarnicola, C., Petitta, M., Scherrer, S. C.,
548 Strasser, U., Winkler, M., Zebisch, M., Cicogna, A., Cremonini, R., Debernardi, A., Faletto, M.,
549 Gaddo, M., Giovannini, L., Mercalli, L., Soubeyroux, J. M., Sušnik, A., Trenti, A., Urbani, S. and
550 Weilguni, V.: Observed snow depth trends in the European Alps: 1971 to 2019, *Cryosphere*, 15(3),
551 1343–1382, doi:10.5194/tc-15-1343-2021, 2021.

552 Mora, J. Á. N., Martín, J. R., García, M. M., de Pablo Davila, F. and Rivas Soriano, L.:
553 Climatological characteristics and synoptic patterns of snowfall episodes in the central Spanish
554 Mediterranean area, *Int. J. Climatol.*, 36(14), 4488–4496, doi:10.1002/joc.4645, 2016.

555 Morán-Tejeda, E., López-Moreno, J. I. and Beniston, M.: The changing roles of temperature and
556 precipitation on snowpack variability in Switzerland as a function of altitude, *Geophys. Res. Lett.*,
557 40(10), 2131–2136, doi:10.1002/grl.50463, 2013.

558 Morán-Tejeda, E., López-Moreno, J. I., Stoffel, M. and Beniston, M.: Rain-on-snow events in
559 Switzerland: Recent observations and projections for the 21st century, *Clim. Res.*, 71(2), 111–125,
560 doi:10.3354/cr01435, 2016.

561 Morán-Tejeda, E., Fassnacht, S. R., Lorenzo-Lacruz, J., López-Moreno, J. I., García, C., Alonso-
562 González, E. and Collados-Lara, A. J.: Hydro-meteorological characterization of major floods in
563 Spanish mountain rivers, *Water (Switzerland)*, 11(12), 2641, doi:10.3390/W11122641, 2019.

564 Muntán, E., García, C., Oller, P., Martí, G., García, A. and Gutiérrez, E.: Reconstructing snow
565 avalanches in the Southeastern Pyrenees, *Nat. Hazards Earth Syst. Sci.*, 9(5), 1599–1612,
566 doi:10.5194/nhess-9-1599-2009, 2009.

567 Musselman, K.N., Addor, N., Vano, J.A. et al. Winter melt trends portend widespread declines in
568 snow water resources. *Nat. Clim. Chang.* 11, 418–424 (2021). <https://doi.org/10.1038/s41558-021-01014-9>

570 Musselman, K. N., Clark, M. P., Liu, C., Ikeda, K. and Rasmussen, R.: Slower snowmelt in a
571 warmer world, *Nat. Clim. Chang.*, 7(3), 214–219, doi:10.1038/nclimate3225, 2017.

572 Nogués-Bravo, D., Araújo, M. B., Lasanta, T. and Moreno, J. I. L.: Climate change in
573 Mediterranean mountains during the 21st century, *Ambio*, 37(4), 280–285, doi:10.1579/0044-
574 7447(2008)37[280:CCIMMD]2.0.CO;2, 2008.

575 Painter, T. H., Berisford, D. F., Boardman, J. W., Bormann, K. J., Deems, J. S., Gehrke, F., Hedrick,
576 A., Joyce, M., Laidlaw, R., Marks, D., Mattmann, C., McGurk, B., Ramirez, P., Richardson, M.,
577 Skiles, S. M. K., Seidel, F. C. and Winstral, A.: The Airborne Snow Observatory: Fusion of
578 scanning lidar, imaging spectrometer, and physically-based modeling for mapping snow water
579 equivalent and snow albedo, *Remote Sens. Environ.*, 184, 139–152, doi:10.1016/j.rse.2016.06.018,
580 2016.

581 Palacios, D. and De Marcos, J.: Geomorphologic Hazards in a Glaciated Granitic Massif: Sierra De
582 Gredos, Spain, in *Geomorphological Hazards in High Mountain Areas*, pp. 285–307, Springer.,
583 1998.

584 Peel, M. C., Finlayson, B. L. and McMahon, T. A.: Updated world map of the Köppen-Geiger
585 climate classification, *Hydrol. Earth Syst. Sci.*, 11(5), 1633–1644, doi:10.5194/hess-11-1633-2007,
586 2007.

587 Pierce, D. W. and Cayan, D. R.: The uneven response of different snow measures to human-induced
588 climate warming, *J. Clim.*, 26(12), 4148–4167, doi:10.1175/JCLI-D-12-00534.1, 2013.

589 Pomeroy, J., Essery, R. and Toth, B.: Implications of spatial distributions of snow mass and melt
590 rate for snow-cover depletion: Observations in a subarctic mountain catchment, *Ann. Glaciol.*, 38,
591 195–201, doi:10.3189/172756404781814744, 2004.

592 R Core Team: A Language and Environment for Statistical Computing, R Found. Stat. Comput., 2,
593 <https://www.R-project.org> [online] Available from: <http://www.r-project.org>, 2020.

594 Revuelto, J., Vionnet, V., López-Moreno, J. I., Lafaysse, M. and Morin, S.: Combining snowpack
595 modeling and terrestrial laser scanner observations improves the simulation of small scale snow
596 dynamics, *J. Hydrol.*, 533, 291–307, doi:10.1016/j.jhydrol.2015.12.015, 2016.

597 Revuelto, J., Billecocq, P., Tuzet, F., Cluzet, B., Lamare, M., Larue, F. and Dumont, M.: Random
598 forests as a tool to understand the snow depth distribution and its evolution in mountain areas,
599 *Hydrol. Process.*, 34(26), 5384–5401, doi:10.1002/hyp.13951, 2020.

600 Robinson, B. G. and Merrill, E. H.: The influence of snow on the functional response of grazing
601 ungulates, *Oikos*, 121(1), 28–34, doi:10.1111/j.1600-0706.2011.19408.x, 2012.

602 Sanmiguel-Vallelado, A., Morán-Tejeda, E., Alonso-González, E. and López-Moreno, J. I.: Effect of
603 snow on mountain river regimes: an example from the Pyrenees, *Front. Earth Sci.*, 11(3)6th January,
604 515–530, doi:10.1007/s11707-016-0630-z, 2017.

605 Sanmiguel-Vallelado, A., Camarero, J. J., Gazol, A., Morán-Tejeda, E., Sangüesa-Barreda, G.,
606 Alonso-González, E., Gutiérrez, E., Alla, A. Q., Galván, J. D. and López-Moreno, J. I.: Detecting
607 snow-related signals in radial growth of *Pinus uncinata* mountain forests, *Dendrochronologia*, 57,
608 125622, doi:10.1016/j.dendro.2019.125622, 2019.

609 Sanmiguel-Vallelado, A., Camarero, J. J., Morán-Tejeda, E., Gazol, A., Colangelo, M., Alonso-
610 González, E. and López-Moreno, J. I.: Snow dynamics influence tree growth by controlling soil
611 temperature in mountain pine forests, *Agric. For. Meteorol.*, 296,
612 doi:10.1016/j.agrformet.2020.108205, 2021.

613 Skamarock, W. C., Klemp, J. B., Dudhia, J. B., Gill, D. O., Barker, D. M., Duda, M. G., Huang, X.-
614 Y., Wang, W. and Powers, J. G.: A description of the Advanced Research WRF Version 3, NCAR
615 Technical Note TN-475+STR, Tech. Rep., (June), 113, doi:10.5065/D68S4MVH, 2008.

616 Sospedra-Alfonso, R. and Merryfield, W. J.: Influences of temperature and precipitation on
617 historical and future snowpack variability over the Northern Hemisphere in the second generation
618 Canadian Earth System Model, *J. Clim.*, 30(12), 4633–4656, doi:10.1175/JCLI-D-16-0612.1, 2017.

619 Sproles, E. A., Nolin, A. W., Rittger, K. and Painter, T. H.: Climate change impacts on maritime
620 mountain snowpack in the Oregon Cascades, *Hydrol. Earth Syst. Sci.*, 17(7), 2581–2597,
621 doi:10.5194/hess-17-2581-2013, 2013.

622 Steiger, R., Scott, D., Abegg, B., Pons, M. and Aall, C.: A critical review of climate change risk for
623 ski tourism, *Curr. Issues Tour.*, 22(11), 1343–1379, doi:10.1080/13683500.2017.1410110, 2019.

624 Sturm, M., Holmgren, J., Liston, G.E.: A Seasonal Snow Cover Classification System for Local to
625 Global Applications. *Journal of Climate* 8, 1261–1283. [https://doi.org/10.1175/1520-0442\(1995\)008<1261:ASSCCS>2.0.CO;2](https://doi.org/10.1175/1520-0442(1995)008<1261:ASSCCS>2.0.CO;2), 1995

627

628 Trigo, R. M., Pozo-Vázquez, D., Osborn, T. J., Castro-Díez, Y., Gámiz-Fortis, S. and Esteban-Parra,
629 M. J.: North Atlantic oscillation influence on precipitation, river flow and water resources in the
630 Iberian Peninsula, *Int. J. Climatol.*, 24(8), 925–944, doi:10.1002/joc.1048, 2004.

631 Trujillo, E. and Molotch, N. P.: Snowpack regimes of the Western United States, *Water Resour.*
632 *Res.*, 50(7), 5611–5623, doi:10.1002/2013WR014753, 2014.

633 Williams, C. J., McNamara, J. P. and Chandler, D. G.: Controls on the temporal and spatial
634 variability of soil moisture in a mountainous landscape: The signature of snow and complex terrain,
635 *Hydrol. Earth Syst. Sci.*, 13(7), 1325–1336, doi:10.5194/hess-13-1325-2009, 2009.

636 Wu, X., Che, T., Li, X., Wang, N. and Yang, X.: Slower Snowmelt in Spring Along With Climate
637 Warming Across the Northern Hemisphere, *Geophys. Res. Lett.*, 45(22), 12,331-12,339,
638 doi:10.1029/2018GL079511, 2018.

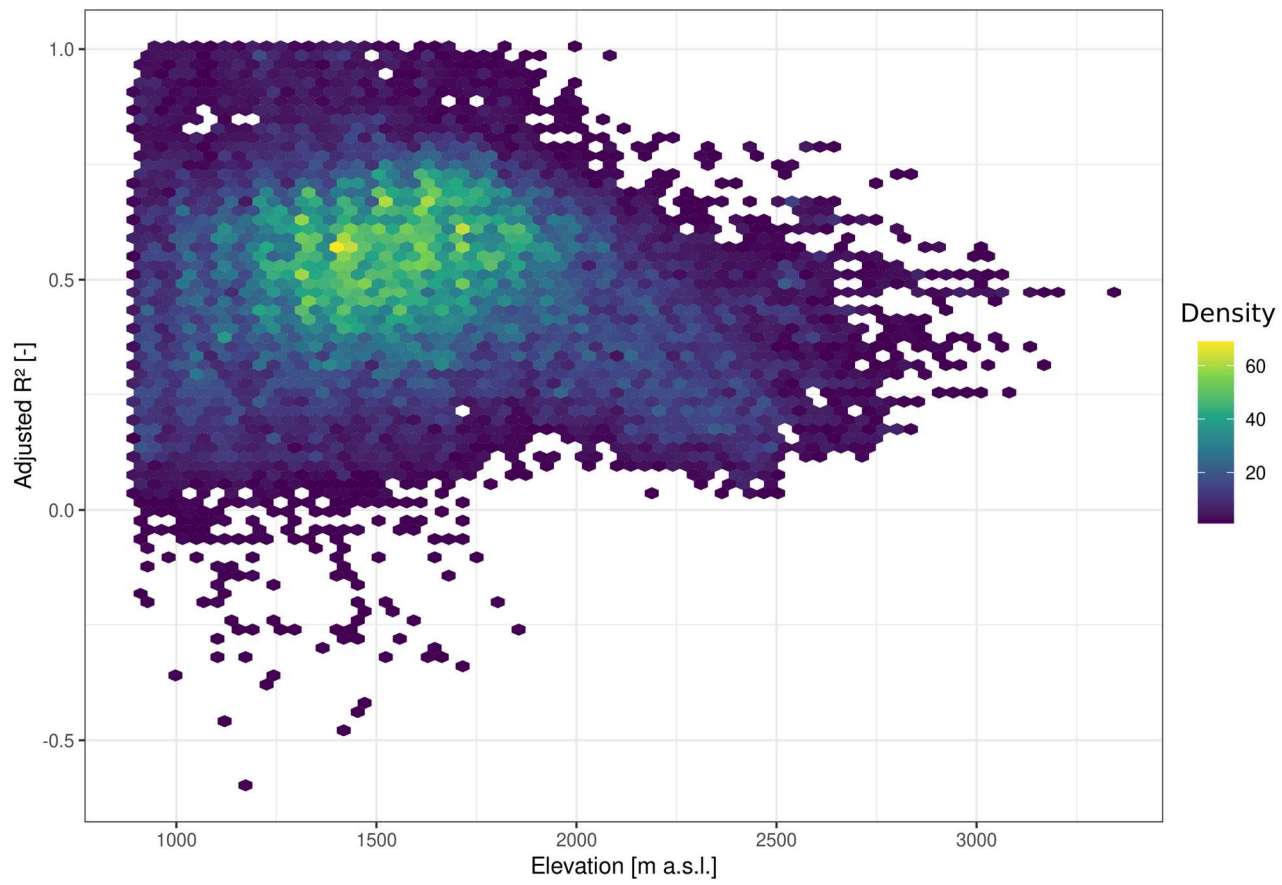
639 Yilmaz, Y., Aalstad, K. and Sen, O.: Multiple Remotely Sensed Lines of Evidence for a Depleting
640 Seasonal Snowpack in the Near East, *Remote Sens.*, 11(5), 483, doi:10.3390/rs11050483, 2019.

641 Zhang, X., Wang, W., Chen, W., Zhang, N. and Zeng, H.: Comparison of seasonal soil microbial
642 process in snow-covered temperate ecosystems of northern China, edited by J. A. Gilbert, *PLoS*
643 *One*, 9(3), e92985, doi:10.1371/journal.pone.0092985, 2014.

644 Zhang, Y., Sherstiukov, A. B., Qian, B., Kokelj, S. V. and Lantz, T. C.: Impacts of snow on soil
645 temperature observed across the circumpolar north, *Environ. Res. Lett.*, 13(4), 044012,
646 doi:10.1088/1748-9326/aab1e7, 2018.

647

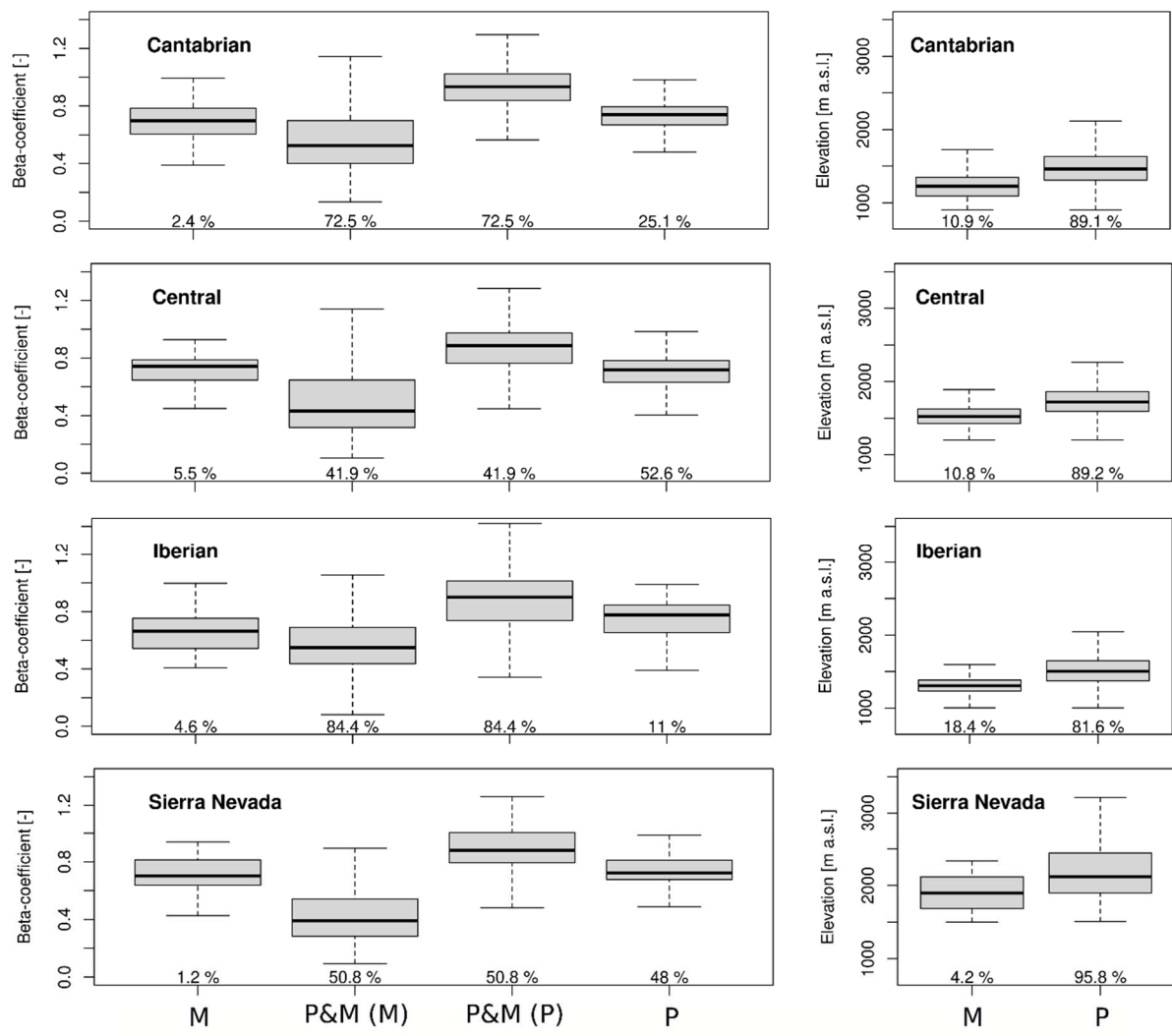
648
649



Supplementary Figure 1: Distribution of the adjusted R^2 values along the elevation range of the Iberian Peninsula.

650

651



Supplementary Figure 2: β -Coefficients for the peak SWE and the melt rate and distribution of the β -coefficients by elevation in the Pyrenees. The figure shows the β -coefficients when one of the predictors is removed from the model ($\beta_x (\beta_y = 0)$) and when both are included with the percentage of the surface under these conditions. The distribution of the β -coefficients with the elevations indicates the elevations where one of the predictors showed a higher β -coefficient, including the situations when one of the predictors was removed from the analysis.

653

654

655